Quantum Simulation of Bound State Scattering

Matteo Turco [1,2,3,6,*] Gonçalo Quinta,[7] João Seixas,[1,2,4,6] and Yasser Omar [1,2,5,6]

[1]*Physics of Information and Quantum Technologies Group, Centro de Física e Engenharia de Materiais Avançados (CeFEMA), Lisbon, Portugal*
[2]*Laboratory of Physics for Materials and Emergent Technologies, Lisbon, Portugal*
[3]*Instituto Superior Técnico, Universidade de Lisboa, Lisbon, Portugal*
[4]*Departamento de Física, Instituto Superior Técnico, Universidade de Lisboa, Lisbon, Portugal*
[5]*Departamento de Matemática, Instituto Superior Técnico, Universidade de Lisboa, Lisbon, Portugal*
[6]*PQI − Portuguese Quantum Institute, Lisbon, Portugal*
[7]*Instituto de Telecomunicações, Lisbon, Portugal*

The last few years have seen rapid development of applications of quantum computation to quantum field theory. The first algorithms for quantum simulation of scattering have been proposed in the context of scalar and fermionic theories, requiring thousands of logical qubits. These algorithms are not suitable to simulate scattering of incoming bound states, as the initial-state preparation relies typically on adiabatically transforming wavepackets of the free theory into wavepackets of the interacting theory. In this paper we present a strategy to excite wavepackets of the interacting theory directly from the vacuum of the interacting theory, allowing the preparation of states of composite particles. This is the first step towards digital quantum simulation of scattering of bound states. The approach is based on the Haag-Ruelle scattering theory, which provides a way to construct creation and annihilation operators of a theory in a full, nonperturbative framework. We provide a quantum algorithm requiring a number of ancillary qubits that is logarithmic in the size of the wavepackets, and with a success probability vanishing at most like a polynomial in the lattice parameters and the energy of the wavepacket. The gate complexity for a single iteration of the circuit is equivalent to that of a time evolution for a fixed time. Furthermore, we propose a complete protocol for scattering simulation using this algorithm. We study its efficiency and find improvements with respect to previous algorithms in the literature.

I. INTRODUCTION

The successes of last few years towards the implementation of quantum algorithms on real platforms are creating growing expectation regarding the opportunities that quantum computation may open in different fields. One prominent area that has been particularly fruitful in providing examples of the potential advantage offered by quantum computation is high-energy physics [1], especially in what concerns data analysis [2–11] and simulations of lattice quantum field theories [12–49]. Such theories have been used for many decades as a tool to numerically investigate several aspects of quantum field theory through the Euclidean path integral approach, which is a powerful tool in its range of applicability but does not cover the whole class of phenomena that require the study of real-time evolution. For such problems the Hamiltonian formulation in Minkowski space-time is the natural framework, but it is hardly approachable with classical computation. For this class of phenomena—and arguably in all the theory of fundamental interactions—scattering events are of special interest since they are essentially the only means we have to access those regimes of physics where quantum field theory is necessary. This work concerns state preparation for digital quantum simulation of scattering.

The prospect of large-scale, fault-tolerant quantum computers, however far they may be in the future, has already started to change our approach to lattice field theory through the seminal papers of Jordan, Lee, and Preskill (JLP) [12,13]. To exploit the potential advantage offered by quantum computers, it is better to formulate the theory

on a space lattice with continuous time rather than on a space-time lattice, as traditionally done. In Refs. [12,13], an efficient quantum algorithm for simulation of scattering in the scalar theory ϕ^4, requiring thousands of logical qubits, is provided and analyzed. The present work aims to contribute to this long-term perspective by making the first step towards digital quantum simulation of scattering events with incoming composite particles. Preparation of bound states is an essential task to ultimately perform simulations of important, real-life collider events, such as proton-proton scattering at the Large Hadron Collider (see Ref. [50] for recent developments in the context of tensor networks and Refs. [51–56] for recent developments in the context of analog quantum simulation).

The same problem was treated in Refs. [57–59], with use of different, albeit equivalent, formulations such as the wavelet basis or the multiparticle decomposition of the Hilbert space. A common feature of these studies is that they all rely on excited states of the associated free theory to prepare wavepackets of the interacting theory. An immediate consequence is that these approaches can be used only for states of the interacting theory that can be obtained by smooth interpolation (typically by an adiabatic transformation) from states of the free theory. This excludes the case of bound states.

Having in mind the framework in Refs. [12,13], we provide in the present work a general strategy to prepare single-particle wavepackets of elementary or composite particles, with lower and upper mass gaps, on a quantum computer. We assume that the preparation of the vacuum state of the interacting theory is available and that we have access to an interpolating operator between the vacuum and the particle we want to create. Once the incoming wavepackets are created, the time evolution and measurements steps of the quantum simulation algorithm proceed as in Refs. [12,13]. The key idea is to use the Haag-Ruelle scattering theory, which is an alternative and complementary approach to the Lehmann-Symanzik-Zimmerman (LSZ) theory. The Haag-Ruelle formalism is of great conceptual importance in the context of axiomatic quantum field theory since it provides a link between the LSZ framework and the Wightman axioms (see, for instance, Ref. [60] for more details). From an operative point of view, its success has been rather limited, on one hand because it is outperformed by the LSZ formalism in the context of perturbation theory and on the other hand because real-time evolution, essential to any scattering theory, is unmanageable with traditional lattice techniques. Quantum computers may offer a new boost to the Haag-Ruelle formalism in terms of operativeness.

The method we propose requires a number of ancillary qubits that is logarithmic in the size of the wavepacket. We provide a quantum circuit with a gate complexity that is equivalent to that of a time evolution for a fixed time, and a certain probability of success. We argue that this probability does not vanish faster than a polynomial in the lattice parameters in the continuum limit. For definiteness, we work here with a single scalar field, because it is an illustrative case and is directly comparable with what is available in the literature. However, the idea holds, *mutatis mutandis*, with other theories as well.

State preparation is typically the most difficult step in digital quantum simulation of scattering, both technically and in terms of complexity. This work provides an innovative approach to the topic and sets the route to the preparation of composite particles. Here we consider the problem of preparing the vacuum only briefly. It is an interesting problem on its own and has already been addressed in other papers [61–66]. For example, one may use the free vacuum preparation and the adiabatic transformation in Ref. [13], with the simplification that no backward time evolution is needed to contain premature wavepacket propagation. We consider this possibility and study its efficiency, with the purpose of providing an estimation of the total scaling of state preparation using our approach. We also compare our approach with the approach of Jordan, Lee, and Preskill, and find that our protocol has a comparable or better scaling than theirs in some cases. If one is interested in only scattering amplitudes, a simpler approach not involving quantum simulation would be the one used in Ref. [67]. However, that approach works only for fixed final states and for processes with a small total number n of ingoing and outgoing particles, as the complexity scales exponentially with n.

We mentioned previously that we rely on the existence of lower and upper mass gaps, but in general we can also have bound states immersed in the continuum of multiparticle states under the condition that they are protected by some symmetry. In this case our strategy is still suitable, with some extra caveats. Fermionic theories do not present extra problems apart from the ones related to encoding of anticommuting degrees of freedom on a qubit system. Gauge theories, as usual, require special attention, not only because of the the well-known issues related to quantum simulation of these theories but also because of the formulation of the Haag-Ruelle theory in the presence of massless particles such as photons. Nevertheless, we assume that with proper care these problems can be solved. For ultrarelativistic particles, the gap closes, and correspondingly the difficulty of creating a particle increases with its momentum. This approach is not suited for the creation of massless particles, for which there is no mass gap.

The rest of this paper is divided into three main sections and an appendix. In Sec. II we very briefly introduce the axiomatic approach to quantum field theory, where the Haag-Ruelle scattering theory is developed. We list the Wightman axioms and introduce basic concepts of the theory. We discuss first a theory with a single elementary particle, and then proceed to a theory in one space dimension

with both an elementary particle and a composite one. We end Sec. II with some remarks on the applicability of our work. In Sec. III we describe how the Haag-Ruelle scattering theory can be used for state preparation in digital quantum simulation. We provide a quantum algorithm for particle creation from the interacting vacuum, and we analyze its complexity and probability of success. In Sec. IV we consider a full protocol for initial-state preparation based on adiabatically preparing the interacting vacuum and then creating wavepackets from it. In the Appendix we discuss the truncation of the field operator in a generic site of the lattice.

II. THE HAAG-RUELLE SCATTERING THEORY

The Haag-Ruelle scattering theory is best developed in the framework of axiomatic quantum field theory. The axiomatic approach provides a rigorous framework to construct a quantum field theory. It is based on a set of axioms formulated by Wightman and incorporates at the same time the principles of quantum mechanics and special relativity. An important feature of this approach is that free and interacting theories are treated on equal terms. In particular, interacting theories are not seen as extensions of free theories obtained by adding interaction terms to a quadratic Hamiltonian. The difference between free theories and interacting theories is mainly of a pragmatical nature, because we can solve and construct explicitly free theories, but for most of the interacting theories the same is not true. For this reason it is quite uncommon to use this approach operatively. In the next two sections we review the Haag-Ruelle formalism, first in the context of a theory with only an elementary particle and then in the context of a theory with bound states.

A. Scalar field without bound states

In this section we give a brief review of the axioms following essentially chapter 9 in Ref. [60]. We consider $d = D - 1$ space dimensions, and we consider here a theory containing a single scalar field, whose dynamics give rise to a single kind of particle of mass m. Examples of such theories include the free scalar field theory and the ϕ^4 theory at weak coupling. The latter has been shown to satisfy the axioms for $d = 1$ and $d = 2$. In the physical case $d = 3$, it is believed to be trivial, i.e., equivalent to a free theory, while for $d \geq 4$, triviality has been proven [68–73] (see also the discussion at the beginning of Sec. 2.1 in Ref. [13]). The free theory is known to satisfy the axioms. The framework can be adapted straightforwardly to the case of a theory with fermionic fields. All that is required is to change commutation relations into anticommutation relations.

It is convenient to divide the whole set of axioms into a few families according to their content. The first one concerns the space of states and the spectral properties of the theory:

(1) *Axiom Ia.* The state space $\mathcal{H}$ of the system is a separable Hilbert space. It carries a unitary representation $U(\Lambda, x)$ (Λ is an element of the homogeneous Lorentz group and x is a space-time coordinate vector) of the proper inhomogeneous Lorentz group (i.e., the Poincaré group). Thus, for all $|\alpha\rangle \in \mathcal{H}$, $|\alpha\rangle \to U(\Lambda, x) |\alpha\rangle$, with the $U(\Lambda, x)$ satisfying the Poincaré algebra

$$U(\Lambda_1, x_1)U(\Lambda_2, x_2) = U(\Lambda_1\Lambda_2, x_1 + \Lambda_1 x_2). \quad (1)$$

(2) *Axiom Ib.* The infinitesimal generators P_μ of the translation subgroup $T(x) = U(\mathbb{1}, x)$ of the Poincaré group have a spectrum p_μ restricted to the forward light cone, $p_0 \geq 0, p^2 \geq 0$.

(3) *Axiom Ic.* There is a unique state $|\Omega\rangle$, the vacuum, with the isolated eigenvalue $p_\mu = 0$ of P_μ.

(4) *Axiom Id.* The theory has a mass gap: the squared-mass operator

$$P^2 = P_\mu P^\mu \quad (2)$$

has an isolated eigenvalue $m^2 > 0$, and the spectrum of P^2 is empty between 0 and m^2. The subspace of $\mathcal{H}$ corresponding to the eigenvalue m^2 carries an irreducible spin-0 representation of the homogeneous Lorentz group. These are the single-particle states of the theory. The remaining spectrum of P^2 is continuous, and it begins at $(2m)^2$.

Clearly the specific form of the generators P_μ depends on the theory at hand, and the generator of translations in time is the Hamiltonian, $P_0 = H$. One-particle states can be labeled according to their momentum and can be written as wavepackets in momentum space

$$|\alpha\rangle_1 = \int d^d k \, \tilde{\psi}(\mathbf{k}) \, |\mathbf{k}\rangle \quad (3)$$

with some wave function $\tilde{\psi}$.

The next family of axioms concerns the operator content of the Hilbert space and establishes what kind of fields appear in the theory:

(1) *Axiom IIa.* An operator-valued (tempered) distribution $\hat{\phi}(x)$ exists such that for any Schwartz test function $f(x)$ the smeared field

$$\phi_f = \int d^D x f(x)\hat{\phi}(x) \quad (4)$$

is an unbounded operator defined on a dense subset $D \subset \mathcal{H}$. Moreover, $\phi_f D \subset D$, allowing the

definition of arbitrary (finite) products of smeared fields.

We recall that a Schwartz function $f(x)$ is infinitely differentiable (i.e., is C^∞) and, together with all its derivatives, falls faster than any power of x as x goes to infinity.

(1) *Axiom IIb.* Under the unitary representation of the Poincaré group $U(\Lambda, x)$ introduced in Axiom Ia, the smeared fields transform as

$$U(\Lambda, x)\phi_f\, U^\dagger(\Lambda, x) = \int d^D y\, f\left[\Lambda^{-1}(y-x)\right] \hat{\phi}(y). \tag{5}$$

(2) *Axiom IIc.* Let f_1 and f_2 be Schwartz functions of compact support: thus, if f_1 vanishes outside a compact space-time region v_1 and f_2 vanishes outside the compact region v_2, and if $x_1 - x_2$ is space-like for all $x_1 \in v_1$, $x_2 \in v_2$, then

$$\left[\phi_{f_1}, \phi_{f_2}\right] = 0. \tag{6}$$

(3) *Axiom IId.* The set of states obtained by applying arbitrary polynomials in the smeared fields ϕ_f (with all possible Schwartz functions f) to the vacuum state $|\Omega\rangle$ is dense in the Hilbert space $\mathcal{H}$.

In Axiom IIa we introduce an important difference with respect to canonical quantization—namely, smeared operators. In a free theory we can identify the operator-valued distribution $\hat{\phi}(x)$ with the familiar field operator. This is not a well-defined operator because the state $\hat{\phi}(x)|\Omega\rangle$ has an infinite norm. To avoid this problem, it is necessary to introduce smearing and treat $\hat{\phi}(x)$ as a distribution. In this way the state $\phi_f|\Omega\rangle$ has a finite norm for any Schwartz function f and ϕ_f is a well-defined (unbounded) operator. Then, by Axiom IIb, we can define

$$\phi_f(x) = e^{iP\cdot x}\phi_f\, e^{-iP\cdot x} = \int d^D y\, f(y-x)\hat{\phi}(y). \tag{7}$$

There are two more axioms of great importance to develop a satisfactory scattering theory:

(1) *Axiom IIIa.* For some one-particle state

$$|\alpha\rangle_1 = \int d^d k\, \tilde{\psi}(\mathbf{k})\, |\mathbf{k}\rangle \tag{8}$$

with discrete eigenvalue m^2 of the squared-mass operator, the smeared field $\phi_f(x)$ has a nonvanishing matrix element from this single-particle state to the vacuum,

$$\langle\Omega|\phi_f(x)|\alpha\rangle_1 \neq 0. \tag{9}$$

(2) *Axiom IIIb* (asymptotic completeness). The Hilbert space $\mathcal{H}_{\text{in}}$ (or $\mathcal{H}_{\text{out}}$) corresponding to multiparticle states of far-separated, freely moving stable particles in the far past (or far future) are unitarily equivalent, and may be identified with the full Hilbert space $\mathcal{H}$ of the system.

It should be noted that Axiom IIIb plays a crucial role in the derivation of the LSZ reduction formula, but here it is somewhat superfluous.

The joint set of eigenvalues of P_μ, labeled by p_μ, is composed of three disconnected subsets (see Fig. 1). There is the vacuum subset, containing only the origin $p_\mu = 0$, the one-particle mass hyperboloid, containing all the p_μ points such that $p^2 = m^2$, and the multiparticle continuum with all the points such that $p^2 \geq 4m^2$. In the two-particle subspace, for instance, the squared-mass operator gives $(p_1 + p_2)^2 = 2m^2 + 2p_1 \cdot p_2$, with $p_1 \cdot p_2 \geq m^2$.

With this in mind we define an operator $\phi_1(x)$ exactly as in Eq. (7) but with a smearing function $f_1(x)$ chosen as the Fourier transform of a function $\tilde{f}_1(p)$ with support in the region

$$am^2 < p^2 < bm^2, \quad 0 < a < 1 < b < 4, \tag{10}$$

sandwiching the one-particle mass hyperboloid. This guarantees that the state $\phi_1(x)|\Omega\rangle$ is a one-particle (and one-particle-only) state, by Axiom IIIa.

Next consider a positive-energy solution of the Klein-Gordon equation,

$$g(\tau, \mathbf{y}) = \int \frac{d^d p}{2E(\mathbf{p})} \tilde{g}(\mathbf{p}) e^{i(\mathbf{p}\cdot\mathbf{y} - E(\mathbf{p})\tau)}, \tag{11}$$

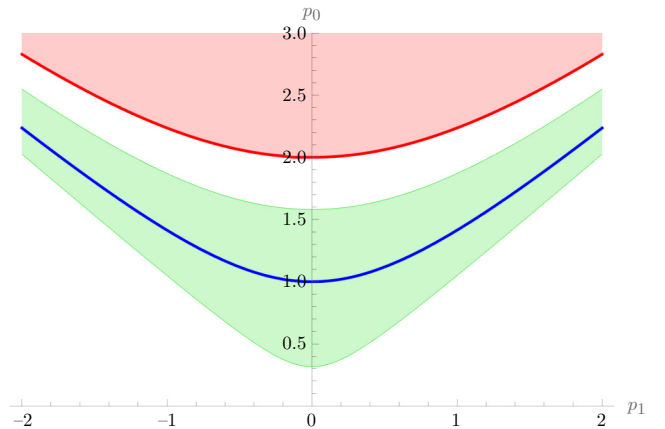$$E(\mathbf{p}) = \sqrt{m^2 + |\mathbf{p}|^2}, \tag{12}$$

FIG. 1. Structure of the spectrum of P_μ with one space dimension. The blue line represents the one-particle mass hyperboloid, the red region is the multiparticle continuum, and the green region is the region defined by $am^2 < p^2 < bm^2$.

and we define the operator

$$\phi_{1,g}(\tau) = -i \int d^d y \left[g(\tau, \mathbf{y}) \frac{\overleftrightarrow{\partial}}{\partial \tau} \phi_1(\tau, \mathbf{y}) \right], \qquad (13)$$

where the double derivative is defined as in

$$A(\tau) \frac{\overleftrightarrow{\partial}}{\partial \tau} B(\tau) = A(\tau) \dot{B}(\tau) - \dot{A}(\tau) B(\tau). \qquad (14)$$

The state $\phi_{1,g}(\tau) |\Omega\rangle$ can be shown to be independent of τ,

$$\frac{d}{d\tau} \phi_{1,g}(\tau) |\Omega\rangle = 0. \qquad (15)$$

This is no longer true in general if we consider multiple applications of such operators at the same time τ, $\phi_{1,g_1}(\tau) \cdots \phi_{1,g_2}(\tau) |\Omega\rangle$, but in this case we can rely on the following theorem (see chapter 9 in Ref. [60] for more details).

Theorem 1 (*Haag asymptotic*). The time-dependent state vector

$$|\Psi, \tau\rangle = \phi_{1,g_1}(\tau) \cdots \phi_{1,g_n}(\tau) |\Omega\rangle \qquad (16)$$

converges strongly in the limit $\tau \to -\infty$ to the *n*-particle in-state

$$|\Psi\rangle_{\text{in}} = |g_1, g_2, \ldots, g_n\rangle_{\text{in}}$$
$$= \int d^d p_1 \ldots d^d p_n \, \tilde{\psi}_{1,g_1}(\mathbf{p}_1) \cdots \tilde{\psi}_{1,g_n}(\mathbf{p}_n)$$
$$\times |\mathbf{p}_1 \cdots \mathbf{p}_n\rangle_{\text{in}}, \qquad (17)$$

with momentum wave functions

$$\tilde{\psi}_{1,g_i}(\mathbf{p}_i) = (2\pi)^{d/2} \frac{\tilde{g}(\mathbf{p}_i) \tilde{f}_1(\mathbf{p}_i)}{\sqrt{2E(p_i)}}. \qquad (18)$$

The convergence rate of the limit $|\Psi, \tau\rangle \to |\Psi\rangle_{\text{in}}$ is $|\tau|^{-d/2}$ in the general case, which includes the case where some or all of the wavepackets $g_1, \ldots, g_n$ overlap with each other and come from the same direction. In this case, the convergence is guaranteed by spreading of the wavepackets to the point where they are so broad that they cease to interact. In practice we consider only wavepackets coming from different directions, and in this case the fast decrease of the Schwartz functions ensures that the convergence rate is faster than any inverse power of $|\tau|$.

The state $|\Psi\rangle_{\text{in}}$ is a Heisenberg state, which implies that it is not to be visualized in general as a state made of n (spatially) well-separated wavepackets. Its form depends on the reference time at which the Heisenberg state and the Schrödinger state coincide. As the reference time, we can choose a moment well before the collision between the wavepackets occurs, in which case we indeed have well-separated wavepackets, or a moment during the collision or later, in which case we can expect to have a complicated state more or less spread in space. The strong convergence of the theorem is to be taken at the same reference time, whether in the far past or not, for both $|\Psi, \tau\rangle$ and $|\Psi\rangle_{\text{in}}$. This reference time should not be confused with the parameter τ appearing in the theorem. But since we will work in the Schrödinger picture, this subtlety is not relevant to us.

Let us see more explicitly what we have stated so far, starting from the state

$$\phi_{1,g}(\tau) |\Omega\rangle = \int d^D x \, \psi(x; \tau) \hat{\phi}(x) |\Omega\rangle, \qquad (19)$$

where

$$\psi(x; \tau) = (2\pi)^d \int d^D p \, \tilde{g}(\mathbf{p}) \tilde{f}_1(p) \frac{p_0 + E(\mathbf{p})}{2E(\mathbf{p})}$$
$$\times e^{-i\tau[E(\mathbf{p}) - p_0]} e^{-ip \cdot x} \qquad (20)$$

is obtained from Eq. (13) after some simple manipulations. For our purposes it is convenient to move to the Schrödinger picture by writing $x = (t, \mathbf{x})$ and plugging

$$\hat{\phi}(x) = e^{itH} \hat{\phi}(0, \mathbf{x}) e^{-iHt} = e^{itH} \hat{\phi}(\mathbf{x}) e^{-iHt} \qquad (21)$$

into Eq. (19). Furthermore, shifting the integration variable in Eq. (19) by $t \to t + \tau$, we get

$$\phi_{1,g}(\tau) |\Omega\rangle = e^{iH\tau} a_\psi^\dagger(\tau) |\Omega\rangle, \qquad (22)$$

$$a_\psi^\dagger(\tau) = \int d^D x \, \psi(t + \tau, \mathbf{x}; \tau) e^{itH} \hat{\phi}(\mathbf{x}) e^{-iHt}. \qquad (23)$$

Let us have a closer look at $\psi(t + \tau, \mathbf{x}; \tau)$. We can rewrite it as

$$\psi(t + \tau, \mathbf{x}; \tau) = (2\pi)^d \int d^d p \, \tilde{g}(\mathbf{p}) \tilde{f}_1'(\mathbf{p}; t) e^{i[\mathbf{x} \cdot \mathbf{p} - \tau E(\mathbf{p})]}, \qquad (24)$$

$$\tilde{f}_1'(\mathbf{p}; t) = \int_{-\infty}^{+\infty} dp_0 \tilde{f}_1(p) \frac{p_0 + E(\mathbf{p})}{2E(\mathbf{p})} e^{-itp_0}. \qquad (25)$$

If, without loss of generality, we assume $f_1(t, \mathbf{x})$ peaked at around $t = 0$, so is $\tilde{f}_1'(\mathbf{p}; t)$. Roughly speaking, the effect of $\tilde{f}_1'(\mathbf{p}; t)$ is to spread $\psi(t + \tau, \mathbf{x}; \tau)$ without changing its position. Therefore, by Eq. (24) we see that $\psi(t + \tau, \mathbf{x}; \tau)$ is essentially a solution of the Klein-Gordon equation moving through space with time τ. When $\tau < 0$, $a_\psi^\dagger(\tau)$ creates a wavepacket at some point along the past trajectory of $\psi(t + \tau, \mathbf{x}; \tau)$. Then, the time evolution operator in Eq. (22) moves it to where $\psi(t + \tau, \mathbf{x}; \tau)$ lies at $\tau = 0$. This accounts for Eq. (15).

Similarly, in the case of two incoming particles, we can write

$$\phi_{1,g_1}(\tau)\phi_{1,g_2}(\tau)\,|\Omega\rangle = e^{iH\tau} a^\dagger_{\psi_1}(\tau) a^\dagger_{\psi_2}(\tau)\,|\Omega\rangle. \quad (26)$$

We can choose $g_1(\tau, \mathbf{y}_1)$ and $g_2(\tau, \mathbf{y}_2)$ such that their wavepackets ψ_1 and ψ_2 are always well separated from each other for $\tau \leq 0$, and are on a collision course for some $\tau > 0$. Then, from Eq. (26), the action of the operators $\phi_{1,g_1}(\tau)\phi_{1,g_2}(\tau)$ on the vacuum is clear: as $\tau \to -\infty$, the two wave functions $\psi_1(t_1 + \tau, \mathbf{x}_1; \tau)$ and $\psi_2(t_2 + \tau, \mathbf{x}_2; \tau)$ are sent far from each other where the two creation operators $a^\dagger_{\psi_1}(\tau)$ and $a^\dagger_{\psi_2}(\tau)$ act undisturbed by each other. Then, the time evolution operator $e^{iH\tau}$ evolves the system forward, making the two wavepackets approach and interact with each other. Let us call r the distance between the regions where $\psi_1(t_1 + \tau, \mathbf{x}_1; \tau)$ and $\psi_2(t_2 + \tau, \mathbf{x}_2; \tau)$ are concentrated at $\tau = 0$. Provided that interactions between particles are short-ranged in the theory, as is the case for gapped theories, we can ignore the interactions occurring between the two wavepackets during the evolution from $\tau = -\infty$ to $\tau = 0$, with error vanishing faster than any inverse power of r. Thus, at the cost of slightly increasing r, we can take $\tau = 0$ in Eq. (26) with excellent precision.

B. Scalar field with bound states

The theory with a single scalar field with interactions $\lambda(\hat\phi^6 - \hat\phi^4)$, in a single space dimension, is a simple example of a quantum field theory displaying bound states. This theory is known to satisfy the Wightman axioms [73], and at weak coupling, it has a single composite particle below the two-particle threshold $2m$. Its mass m_b can be computed perturbatively [74–76] as

$$m_b = 2m \left[1 - \frac{9}{8}\left(\frac{\lambda}{m^2}\right)^2 + O(\lambda^3) \right]. \quad (27)$$

The bare mass $m_0(\lambda)$ can be set such that $m = m(m_0(\lambda), \lambda)$ is fixed. We notice at this point that Axiom Id should be modified in an obvious way to accommodate the composite particle with mass m_b. This is a well-controlled model that is perfect to see in a simple and explicit way how to treat bound states in the Haag-Ruelle formalism. The last ingredient we need to know is that the field $:\hat\phi^2:(x)$ interpolates between the vacuum and one-particle states of the composite particle [76]. The Wick ordering $:\cdot:$ is necessary in the continuum to avoid divergences of $\hat\phi^2(x)$, but on the lattice it amounts to a constant, finite shift. This is completely irrelevant to our purposes as can be easily seen. Let $\hat\Phi(x)$ denote either $\hat\phi(x)$ or $:\hat\phi^2:(x)$. Then, if we shift it by a constant A and smear it with the function ψ in

Eq. (20), we obtain

$$\int d^D x\, \hat\Phi(x)\psi(x;\tau)\,|\Omega\rangle + A \int d^D x\, \psi(x;\tau)\,|\Omega\rangle. \quad (28)$$

The second term is proportional to $\tilde{f}_1(0)$, which is zero by construction.

The joint spectrum of $P_0 = H$ and P_1 is depicted in Fig. 2. Starting from this picture, we find that the Haag-Ruelle theory discussed in the previous section holds equally well to obtain wavepackets of the elementary particle with mass m, or wavepackets of the composite particle with mass m_b. If we want to have an elementary particle, we use the interpolating field $\hat\phi(x)$, a smearing function $f_1(x)$, with Fourier transform $\tilde{f}_1(p)$ sandwiching the hyperboloid of mass m, and a solution $g(x)$ of the Klein-Gordon equation to build the operator $\phi_{1,g}(\tau)$ of Eq. (13) as before. If, on the other hand, we want to obtain a composite particle, we use the interpolating field $:\hat\phi^2:(x)$, a smearing function $f_b(x)$, with Fourier transform $\tilde{f}_b(p)$ sandwiching the hyperboloid of mass m_b, and a solution $h(x)$ of the Klein-Gordon equation to obtain the operator

$$\phi_{b,h}(\tau) = -i \int_{-\infty}^{+\infty} d\mathbf{y} \left[h(\tau, \mathbf{y}) \overset{\leftrightarrow}{\frac{\partial}{\partial\tau}} \phi_b(\tau, \mathbf{y}) \right], \quad (29)$$

where

$$\phi_b(x) = \int d^2 y\, f_b(y - x) :\hat\phi^2:(y). \quad (30)$$

Then everything proceeds as before. A useful remark is that the field $\hat\phi(x)$ does not interpolate between the vacuum and one-particle states of the composite kind, and vice
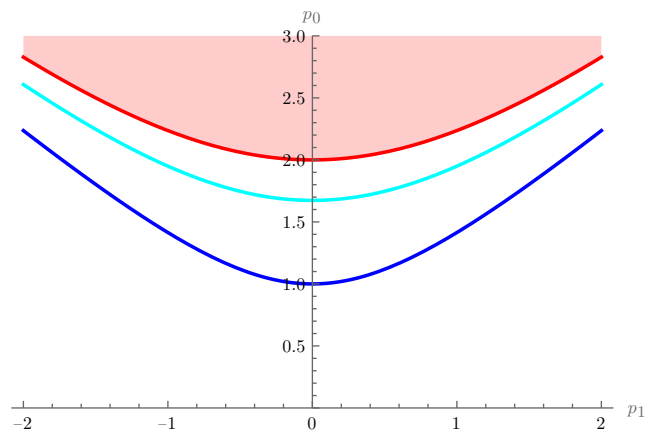

FIG. 2. Structure of the spectrum of P_μ in the theory $\lambda(\hat\phi^6 - \hat\phi^4)$. The blue line represents the mass hyperboloid of elementary particles, the cyan line represents the mass hyperboloid of two-particle bound states, and the red region is the multiparticle continuum.

versa, $: \hat{\phi}^2 : (x)$ does not interpolate between the vacuum and one-particle states of the elementary kind. In the formulae, if $|\alpha_1\rangle$ is an elementary one-particle state and $|\alpha_b\rangle$ is a composite one-particle state, we have

$$\langle \alpha_1 | : \hat{\phi}^2 : (x) |\Omega\rangle = 0 = \langle \alpha_b | \hat{\phi}(x) |\Omega\rangle. \quad (31)$$

The first equality holds because the one-particle sector of the elementary kind is spanned by vectors of the form $\phi_1(x) |\Omega\rangle$. Then the matrix element $\langle \alpha_1 | : \hat{\phi}^2 : (x) |\Omega\rangle$ is an integral containing $\langle \Omega | \hat{\phi} \, \hat{\phi} \, \hat{\phi} |\Omega\rangle$, which is zero because the Hamiltonian contains only even powers of the field $\hat{\phi}$. A similar argument leads to $\langle \alpha_b | \hat{\phi}(x) |\Omega\rangle = 0$. As a consequence of the equalities in Eq. (31), $\tilde{f}_1$ and $\tilde{f}_b$ are allowed to have supports intersecting both hyperboloids of mass m and m_b.

We conclude this section with some remarks on the validity of the theory just described. In general, we can have bound states whose mass falls above the two-particle threshold of lighter particles, on the condition that they are protected by some symmetry (internal quantum numbers). In this case the symmetry selects a sector of the Hilbert space, and when we restrict the mass-squared operator to this sector, the mass of the composite particle appears as a discrete point in the spectrum of P^2 again.

The Haag asymptotic theorem critically depends on two assumptions:

(1) There exists a lower and an upper mass gap for the particle we want to create in such a way that it is possible to sandwich the mass hyperboloid corresponding to such a particle.

(2) We have access to an operator interpolating between the vacuum and one-particle states of the particle we want to create.

Clearly, studying these two conditions strongly depends on the theory under consideration and can be very difficult, but we can use standard techniques of lattice quantum field theory to study these properties model by model, or the Bethe-Salpeter equation as done in Refs. [74–76]. Smearing a field operator in time can be avoided if we have at our disposal an operator that does not couple the vacuum to multiparticle states (as happens for free theories). For a bound state whose mass is immersed in the continuum of other particles, we also need to ensure that the interpolating operator couples only to the sector where the bound state lives, in a way similar to the reasoning leading to Eq. (31). As an example, consider a theory where we have a composite particle with spin 0 and mass m (a pion), and another composite particle with spin 1/2 and mass $M > 2m$ (a proton). These two particles are made of the same underlying elementary fields, but the difference in spin should make it easy to build interpolating fields from the vacuum to each of the two particles without crossing, even though the

heavier particle has mass in the continuum of the lighter one.

III. STATE PREPARATION USING THE HAAG-RUELLE THEORY

In the following we assume that all of this holds as an approximation on the lattice. The Haag-Ruelle scattering theory was developed for spin systems in Ref. [77] and for Euclidean lattice field theory in Ref. [78]. Detailed studies of the effects of latticization on applications for quantum simulation will be the subject of future work.

From now on we take $\tau = 0$, $\psi(t, \mathbf{x}) = \psi(t, \mathbf{x}; 0)$, as given in Eq. (20), and

$$a_\psi^\dagger = \sum_{\mathbf{x}} a^d \int_{-\infty}^{+\infty} dt \, \psi(t, \mathbf{x}) e^{iHt} \hat{\phi}(\mathbf{x}) e^{-iHt}. \quad (32)$$

We want to prepare the state $a_{\psi_1}^\dagger a_{\psi_2}^\dagger |\Omega\rangle$, with ψ_1 and ψ_2 well separated. Because of this, we can focus on one wavepacket at a time, so in the following we will see how to implement the operator $a_\psi^\dagger$ on a quantum computer. In Eq. (20), we choose $\tilde{g}$ peaked at around $\bar{\mathbf{p}}$ with support of size δ_p and $\tilde{f}_1(p)$ peaked at around $(\bar{E}, \bar{\mathbf{p}})$ with support of size δ_E in the p_0 direction and δ_p in the other directions, with $\bar{E} = E(\bar{\mathbf{p}})$. Also, we can take $\delta_E = O(m)$. First we truncate the integration over t and the summation over $\mathbf{x}$ around the space-time region where ψ is significantly different from zero, which, since ψ is a Schwartz function, introduces an error vanishing faster than any power as the hypervolume of the region is increased. We label the space points in this region by $\mathbf{x}_1, \ldots, \mathbf{x}_S$ and we approximate the integral with a sum over time points $t_1, \ldots, t_N$ with spacing δ_t. By the uncertainty principle, the linear size of ψ over space is proportional to $1/\delta_p$, and $t_N - t_1$ is proportional to $1/\delta_E = O(1/m)$. Thus, as an approximation of $a_\psi^\dagger$, we have

$$\bar{a}_\psi^\dagger = \sum_{i=1}^{N} \sum_{j=1}^{S} a^d \delta_t \psi(t_i, \mathbf{x}_j) e^{iHt_i} \hat{\phi}(\mathbf{x}_j) e^{-iHt_i}$$

$$= \sum_{i=1}^{N} \hat{\phi}_\psi(t_i). \quad (33)$$

We work in the field basis [12,13,79], where the operator $\hat{\phi}(\mathbf{x})$ is diagonal. If k qubits are dedicated to the lattice site $\mathbf{x}$, then $\hat{\phi}(\mathbf{x})$ is implemented by a linear combination of Z Pauli matrices,

$$\hat{\phi}(\mathbf{x}) = \frac{\phi_{\max}}{2^k - 1} \sum_{i=0}^{k-1} 2^i \sigma_{(\mathbf{x},i)}^z. \quad (34)$$

The effects of truncating and discretizing the spectrum of $\hat{\phi}(\mathbf{x})$ were studied in Refs. [12,13,79], where it is

also shown that it is enough to take k quite small in a broad range of situations. The operator (34) is not unitary but can be implemented with linear combination of unitaries (LCU) [80]. Furthermore, the operator $\bar{a}_\psi^\dagger$ can be implemented with LCU as well, with probability of success

$$\rho = \left(\frac{|| \bar{a}_\psi^\dagger |\Omega\rangle ||}{\alpha} \right)^2, \tag{35}$$

$$\alpha = \phi_{\max} \sum_{i=1}^N \sum_{j=1}^S a^d \delta_t |\psi(t_i, \mathbf{x}_j)|. \tag{36}$$

It is not easy to determine ρ exactly (more is said on this at the end of this section), but one could use, for example, the techniques described in Ref. [81] to find numerical estimates for it. Then one would have to repeat state preparation $O(1/\rho)$ times to get the desired initial state, or, alternatively, one could apply amplitude amplification [81] to obtain a quadratic speedup at the expense of a larger circuit depth. Typically, we need to prepare two incoming wavepackets. If we denote by ρ_1 and ρ_2 the probabilities of obtaining the two wavepackets, the total probability is given by $\rho = \rho_1 \rho_2$. Generalization to more than two wavepackets is straightforward.

Before moving on, we remarks on how to implement the bound-state creation operator (29). The discussion goes along the line described so far, except that now, instead of Eq. (34), we have to use the operator

$$\hat{\phi}(\mathbf{x})^2 = \left(\frac{\phi_{\max}}{2^k - 1} \right)^2 \sum_{i,j=0}^{k-1} 2^{i+j} \sigma_{(\mathbf{x},i)}^z \sigma_{(\mathbf{x},j)}^z \tag{37}$$

up to a shift. We are free to choose this shift in such a way as to eliminate the terms with $i = j$ in Eq. (37), which are proportional to $\mathbb{1}$. In this way, instead of α in Eq. (36), we obtain

$$\alpha_b \approx \frac{2}{3} \phi_{\max}^2 \sum_{i=1}^N \sum_{j=1}^S a^d \delta_t |\psi(t_i, \mathbf{x}_j)|. \tag{38}$$

A. Circuit description

We want to give a high-level description of a circuit implementing $\bar{a}_\psi^\dagger$, so we focus only on the dependence on the lattice sites and the time to keep the discussion concise. We take a register of $N_a = \lceil \log_2(kNS) \rceil$ ancillary qubits and we label the computational basis as $|t_i, \mathbf{x}_j\rangle$, with $i = 1, \dots, N$ and $j = 1, \dots, S$.

We define operators V_ψ and V'_ψ such that

$$V_\psi |0\rangle^{\otimes N_a} = \frac{1}{\sqrt{\|\psi\|_1}} \sum_{i=1}^N \sum_{j=1}^S \sqrt{a^d \delta_t \psi(t_i, \mathbf{x}_j)} |t_i, \mathbf{x}_j\rangle, \tag{39}$$

$$V_\psi'^\dagger |0\rangle^{\otimes N_a} = \frac{1}{\sqrt{\|\psi\|_1}} \sum_{i=1}^N \sum_{j=1}^S \left(\sqrt{a^d \delta_t \psi(t_i, \mathbf{x}_j)} \right)^* |t_i, \mathbf{x}_j\rangle. \tag{40}$$

Then the circuits in Fig. 3 implement the operator $\bar{a}_\psi^\dagger$ written in Eq. (33) up to a normalization factor and when the state $|0\rangle^{\otimes N_a}$ is obtained by measurement of the ancillary register. In general we have $t_1 < 0$, $t_N > 0$, and $t_i - t_{i+1} = -\delta_t$; therefore, the sequence of time evolution operators appearing in Fig. 3(a) consists of a backward evolution for time $|t_1|$, followed by N steps forward, each one of time δ_t for a total of $t_N - t_1$, and by a final backward evolution for time t_N. In Fig. 3(b) we notice that controlling only each $\hat{\phi}$ is equivalent to controlling $e^{-iHt_i} \hat{\phi} e^{iHt_i}$ because $e^{-iHt_i} e^{iHt_i} = \mathbb{1}$. To prepare two wavepackets, we can take two ancillary registers, apply in sequence the circuit in Fig. 3, one for each wavepacket, and measure both ancillary registers at the end.

B. Complexity

We show that the complexity in Fig. 3(a) is dominated by the sequence of time evolutions. We do not want to discuss here how to implement the time evolution, as this is not in the scope of this work. Moreover, we take $k = \tilde{O}(1)$.

The sequence of operators $\Phi(t_1), \dots, \Phi(t_N)$ requires $O(kSN) = \tilde{O}(SN)$ gates, as well as the operators V and V', which basically provide generic state preparation on N_a qubits, and we have $S < \mathcal{V}$. We can estimate the error introduced by discretizing the integral over t, and hence how large N needs to be, in the following way. We take $t_0 = t_1 - \delta_t/2$ and $T = t_N - t_1 + \delta_t$. Then we split the integral from t_0 to $t_0 + T$ into N integrals in the following way:

$$\int_{t_0}^{t_0+T} \psi(t, \mathbf{x}) e^{iHt} \hat{\phi}(\mathbf{x}) e^{-iHt} dt$$

$$= \sum_{i=1}^N \int_{t_i - \frac{\delta_t}{2}}^{t_i + \frac{\delta_t}{2}} \psi(t, \mathbf{x}) e^{iHt} \hat{\phi}(\mathbf{x}) e^{-iHt} dt$$

$$= \sum_{i=1}^N \int_{-\frac{\delta_t}{2}}^{\frac{\delta_t}{2}} \psi(t_i + t, \mathbf{x}) e^{iHt_i} e^{iHt} \hat{\phi}(\mathbf{x}) e^{-iHt} e^{-iHt_i} dt, \tag{41}$$

where from the second line to the third line we have shifted the integration variable, $t \to t + t_i$. We expand $e^{iHt} \hat{\phi}(\mathbf{x}) e^{-iHt}$ using the formula

$$e^A B e^{-A} = B + [A, B] + \frac{1}{2} [A, [A, B]] + \cdots \tag{42}$$

and we expand $\psi(t_i + t, \mathbf{x})$ using the Taylor expansion around $t = 0$ up to order t^2. Odd orders in t do not contribute because the integration domain is symmetric around
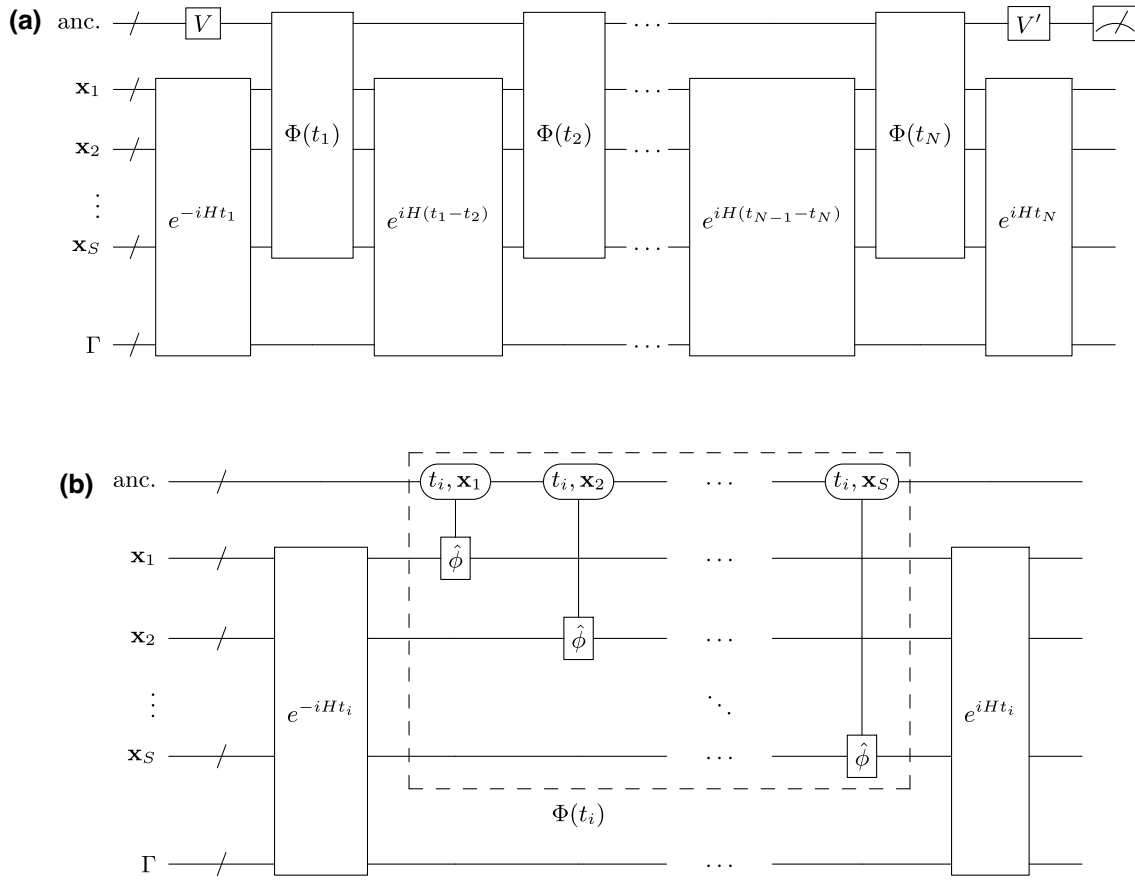
FIG. 3.   Description of the circuit implementing $\bar{a}_\psi^\dagger$. The slash at the beginning of each line means that the line represents a register of qubits: "anc." is the ancillary register of N_a qubits, $\mathbf{x}_i$ is the register of k qubits dedicated to the site $\mathbf{x}_i$, and Γ is the set of qubits dedicated to the rest of the lattice. (a) Circuit 1: High-level overview of the circuit implementing $\bar{a}_\psi^\dagger$. The operators $\Phi(t_i)$ are described in the circuit in (b). (b) Circuit 2: Overview of the operator implementing $\hat{\phi}_\psi(t_i)$. The symbol connecting $\hat{\phi}$ in a squared box to the rounded box containing $t_i, \mathbf{x}_j$ represents the operator $\hat{\phi}(\mathbf{x})$ controlled on the state $|t_i, \mathbf{x}_j\rangle$.

zero. The leading order gives us exactly the operators appearing in Eq. (33). We use the spectral norm of the next to leading order to estimate the error due to discretization and we apply the triangular inequality:

$$\epsilon = \frac{\delta_t^3}{24}\|\sum_{i=1}^{N} e^{iHt_i}\left(\ddot{\psi}(t_i,\mathbf{x})\hat{\phi}(\mathbf{x}) + 2i\dot{\psi}(t_i,\mathbf{x})[H,\hat{\phi}(\mathbf{x})] - \psi(t_i,\mathbf{x})\left[H,[H,\hat{\phi}(\mathbf{x})]\right]\right)e^{-iHt_i}\|$$

$$\leq \frac{\delta_t^2}{24}\left(\sum_{i=1}^{N}\delta_t|\ddot{\psi}(t_i,\mathbf{x})|\|\hat{\phi}(\mathbf{x})\| + 2\sum_{i=1}^{N}\delta_t|\dot{\psi}(t_i,\mathbf{x})|\|[H,\hat{\phi}(\mathbf{x})]\| + \sum_{i=1}^{N}\delta_t|\psi(t_i,\mathbf{x})|\|\left[H,[H,\hat{\phi}(\mathbf{x})]\right]\|\right). \tag{43}$$

The dominant contribution is given by the term with $\left[H,[H,\hat{\phi}(\mathbf{x})]\right]$, and the quantity

$$\sum_{i=1}^{N}\delta_t|\psi(t_i,\mathbf{x})| \tag{44}$$

is approximately a constant independent of the lattice and the precision. Finally, given that $T = \delta_t N$, we have

$$N = \tilde{O}\left(\frac{T}{\sqrt{\epsilon}}\sqrt{\|\left[H,[H,\hat{\phi}(\mathbf{x})]\right]\|}\right). \tag{45}$$

If we use a first-order Suzuki-Trotter formula to implement the time evolution, we need [82]

$$N_{\text{ST}} = O\left(\frac{T^2}{\epsilon} \|[H_\phi, H_\pi]\|\right) \tag{46}$$

Trotter steps to keep the error below ϵ. As one may check by looking at Eqs. (47) and (48), the commutator $[H_\phi, H_\pi]$

$$\left[H, [H, \hat{\phi}(\mathbf{x})]\right] = \frac{1}{a^2} \sum_{i=1}^{d} \left[2\hat{\phi}(\mathbf{x}) - \hat{\phi}(\mathbf{x} + \hat{\mathbf{r}}_i) - \hat{\phi}(\mathbf{x} - \hat{\mathbf{r}}_i)\right] + m_0^2 \hat{\phi}(\mathbf{x}) + \frac{\lambda_0}{3!}\hat{\phi}(\mathbf{x})^3, \tag{47}$$

$$[H_\phi, H_\pi] = i \sum_{\mathbf{x}} a^d \left[\frac{1}{a^2} \sum_{j=1}^{d} \left(\hat{\phi}(\mathbf{x})\hat{\pi}(\mathbf{x}) + \hat{\phi}(\mathbf{x} + \hat{\mathbf{r}}_j)\hat{\pi}(\mathbf{x} + \hat{\mathbf{r}}_j) - \hat{\phi}(\mathbf{x} + \hat{\mathbf{r}}_j)\hat{\pi}(\mathbf{x}) - \hat{\phi}(\mathbf{x})\hat{\pi}(\mathbf{x} + \hat{\mathbf{r}}_j) - \frac{i}{a^d}\right) \right.$$

$$\left. + \frac{m_0^2}{2}\left(2\hat{\phi}(\mathbf{x})\hat{\pi}(\mathbf{x}) - \frac{i}{a^d}\right) + \frac{\lambda_0}{12}\left(2\hat{\phi}^3(\mathbf{x})\hat{\pi}(\mathbf{x}) - \frac{3i}{a^d}\hat{\phi}(\mathbf{x})^2\right)\right]. \tag{48}$$

C. Success probability

Here we want to show what to expect regarding the probability of success. We write it again here:

$$\rho = \left(\frac{\|\bar{a}_\psi^\dagger |\Omega\rangle\|}{\alpha}\right)^2, \tag{49}$$

$$\alpha = \phi_{\max} \sum_{i=1}^{N} \sum_{j=1}^{S} a^d \delta_t |\psi(t_i, \mathbf{x}_j)|, \tag{50}$$

$$\bar{a}_\psi^\dagger |\Omega\rangle = \sum_{i=1}^{N} \sum_{j=1}^{S} a^d \delta_t \psi(t_i, \mathbf{x}_j) e^{it_i H} \hat{\phi}(\mathbf{x}_j) |\Omega\rangle. \tag{51}$$

Near the continuum limit, $\|\bar{a}_\psi^\dagger |\Omega\rangle\|^2$ should approach its continuum value

$$Z \int d^d p \, \frac{|\tilde{g}(\mathbf{p})\tilde{f}_1(E(\mathbf{p}), \mathbf{p})|^2}{2E(\mathbf{p})}, \tag{52}$$

where Z depends on the normalization of the field operator $\hat{\phi}(\mathbf{x})$. The summation in α can be approximated by an integral, so we have

$$\rho \sim \frac{Z}{\phi_{\max}^2} \frac{\int d^d p \, \frac{|\tilde{g}(\mathbf{p})\tilde{f}_1(E(\mathbf{p}), \mathbf{p})|^2}{2E(\mathbf{p})}}{\left(\int d^D x \, |\psi(x)|\right)^2}. \tag{53}$$

Since $\tilde{g}(\mathbf{p})\tilde{f}_1(p_0, \mathbf{p})$ has support of size δ_E in the p_0 direction and support of size δ_p in the other directions, we

scales with the total size of the lattice, as it involves a summation over all the sites, while $\left[H, [H, \hat{\phi}(\mathbf{x})]\right]$ involves only a few neighbors of $\mathbf{x}$. Thus, N_{ST} clearly dominates over N even if we consider higher-order product formulae. This shows that the complexity is determined by the time evolution.

For the ϕ^4 theory, we have

have

$$\left(\int d^D x \, |\psi(x)|\right)^2 \sim \frac{1}{\delta_E \delta_p^d} \int d^D x \, |\psi(x)|^2$$

$$= \frac{1}{\delta_E \delta_p^d} \int d^D p \, \left|\tilde{g}(\mathbf{p})\tilde{f}_1(p)\frac{p_0 + E(\mathbf{p})}{2E(\mathbf{p})}\right|^2. \tag{54}$$

In the limit $\delta_p \to 0$ we can approximate $\tilde{g}$ with a δ function centered in $\bar{\mathbf{p}}$, and recalling $\bar{E} = E(\bar{\mathbf{p}})$, we obtain

$$\frac{\int d^d p \, \frac{|\tilde{g}(\mathbf{p})\tilde{f}_1(E(\mathbf{p}), \mathbf{p})|^2}{2E(\mathbf{p})}}{\left(\int d^D x \, |\psi(x)|\right)^2} \sim \frac{\delta_p^d}{\bar{E}} \frac{\delta_E |\tilde{f}_1(\bar{E}, \bar{\mathbf{p}})|^2}{\int_{-\infty}^{+\infty} dp_0 \, |\tilde{f}_1(p_0, \bar{\mathbf{p}})\frac{p_0 + \bar{E}}{2\bar{E}}|^2}$$

$$\sim \frac{\delta_p^d}{\bar{E}} \tag{55}$$

and

$$\rho = O\left(\frac{Z}{\phi_{\max}^2} \frac{\delta_p^d}{\bar{E}}\right). \tag{56}$$

We now turn our attention to the factor $Z/\phi_{\max}^2$. Set

$$\sigma_E = \sqrt{\langle \psi_E | \hat{\phi}(0)^2 | \psi_E \rangle}, \tag{57}$$

$$\sigma_0 = \sqrt{\langle \Omega | \hat{\phi}(0)^2 | \Omega \rangle}, \tag{58}$$

where $|\psi_E\rangle$ is a state with maximum energy E and E is the energy of the process being simulated. In Ref. [13], as a

consequence of Chebyshev's inequality, it is shown that

$$\phi_{\max} = O\left(\sigma_E \sqrt{\frac{\mathcal{V}}{\epsilon_{\text{trunc}}}}\right), \tag{59}$$

where ϵ_{trunc} is the error due to truncation of the spectrum of $\hat{\phi}(\mathbf{x})$. In the field representation we have

$$|\psi_E\rangle = \int_{-\infty}^{+\infty} d\phi_1 \cdots \int_{-\infty}^{+\infty} d\phi_{\mathcal{V}} \, \psi_E(\phi_1, \ldots, \phi_{\mathcal{V}})$$
$$\times |\phi_1 \cdots \phi_{\mathcal{V}}\rangle, \tag{60}$$

where $1, \ldots, \mathcal{V}$ is some labeling of the lattice sites. It is well known [83] that $\psi_E(\phi_1, \ldots, \phi_{\mathcal{V}})$ decays rapidly (exponentially or more) outside the classically forbidden region $V(\phi_1, \ldots, \phi_{\mathcal{V}}) > E$, where $V(\phi_1, \ldots, \phi_{\mathcal{V}})$ is the potential associated with the Hamiltonian H. From the discussion in the Appendix it is clear that we can improve the bound (59) to

$$\phi_{\max} = O\left(\sigma_E \sqrt{\mathcal{V}} + \log_2 \frac{\mathcal{V}}{\epsilon_{\text{trunc}}}\right). \tag{61}$$

Moreover, from the analysis in Ref. [13] it follows that (at most) $\sigma_E = O(\sqrt{E}\sigma_0)$, and thus, ignoring the logarithmic contribution, we have

$$\phi_{\max} = O\left(\sigma_0 \sqrt{E\mathcal{V}}\right). \tag{62}$$

We can use the Källen-Lehmann representation of the two-point function in the continuum to estimate σ_0. We have

$$\langle\Omega| \hat{\phi}(x)\hat{\phi}(y) |\Omega\rangle = Z\Delta_+(x-y, m^2)$$
$$+ \int_{4m^2}^{+\infty} \rho(\mu)\Delta_+(x-y, \mu)d\mu, \tag{63}$$

where $\rho(\mu) \geq 0$ is the so-called spectral function and

$$\Delta_+(x, \mu) = \frac{1}{(2\pi)^d} \int \frac{d^d p}{2\sqrt{|\mathbf{p}|^2 + \mu}} e^{-ip \cdot x}. \tag{64}$$

In renormalizable models such as ϕ^4, the spectral function is known to decay as $1/\mu$ at all orders of perturbation theory, ensuring the convergence of the integral in Eq. (63). Therefore, we may assume that, at coincident points $x = y$, the behavior of the two-point function is determined by $\Delta_+(0, m^2)$, which diverges logarithmically for $d = 1$ and linearly and quadratically (apart from logarithmic factors) for $d = 2$ and $d = 3$, respectively. As $1/a$ is a natural cutoff

on the lattice, we may conclude that

$$\phi_{\max} = \tilde{O}\left(\sqrt{\frac{EZ\mathcal{V}}{a^{d-1}}}\right), \tag{65}$$

where we use the notation $\tilde{O}(\cdot) = O(\cdot \text{polylog}(\cdot))$, and consequently

$$\rho \gtrsim \frac{a^{d-1}\delta_p^d}{\mathcal{V}E\bar{E}}, \tag{66}$$

up to logarithmic factors. As we are interested in the continuum limit, the dominant factor is $a^{d-1}/\mathcal{V}$. From the discussion in the Appendix, we expect this bound to be quite loose. For the perturbative ϕ^4 theory, for instance, we can replace $\mathcal{V}$ with $\sqrt{\mathcal{V}}$.

IV. COMPARISON WITH THE JLP ALGORITHM

In this section we compare the complexity scaling of our strategy with the complexity scaling of the JLP strategy [12,13] in the case when both methods are applicable—that is, when we want to prepare elementary particles. We consider only the ϕ^4 theory. The settings in the two cases are very similar and a comparison is immediate.

The JLP algorithm can be summarized in five steps:

(1) Free vacuum preparation
(2) Creation of free wavepackets
(3) Adiabatic transformation of the free wavepackets into interacting wavepackets
(4) Time evolution
(5) Measurements

As stated in Sec. I, our strategy requires the preparation of the interacting vacuum. While other techniques, such as variational approaches, might be more suitable in practice, to study the complexity we choose here to do the following:

(1) Free vacuum preparation
(2) Adiabatic transformation of the free vacuum into the interacting vacuum
(3) Creation of interacting wavepackets
(4) Time evolution
(5) Measurements

Steps 4 and 5 are the same in the two approaches, and in both cases the bottleneck of complexity is in the initial-state preparation—steps 1, 2, and 3—so we focus on these steps only. We consider here the case of two particles in the initial state. As the complexity depends on the success probability, simulating scattering between three or more incoming particles becomes more and more inefficient in our approach, and is of little or no practical interest in

general. We assume the reader is familiar with Ref. [13], especially with Secs. 3.2 and 4.2. We do not want to discuss the details of how time evolution is implemented, although it may have an impact on complexity. Our goal is to give a rough estimate, certainly not exhaustive, and to compare it with the results obtained by Jordan, Lee, and Preskill. To this end and following their approach, we assume we can implement time evolution with a kth-order Suzuki-Trotter formula with large k. The gate cost for time t on a lattice of $\mathcal{V}$ sites is

$$(\mathcal{V}t)^{1+\frac{1}{2k}}, \tag{67}$$

which we indicate as

$$(\mathcal{V}t)^{1+o(1)} \tag{68}$$

to simplify the presentation. The little-o notation is used also to include logarithmic factors implicit in the $\tilde{O}$ notation.

The most-time-consuming parts are typically the free vacuum preparation and the adiabatic transformation. The complexity for the free vacuum preparation, using the Kitaev-Webb method [84,85], is $O(\mathcal{V}^{2.376})$. This exponent is determined by the classical computation of the LDL decomposition of the covariance matrix. The quantum circuit has a depth of $\tilde{O}(\mathcal{V}^2)$ and requires $O(\log_2 \mathcal{V})$ ancillary qubits [85].

The adiabatic transformation of the wavepackets requires a modification with respect to a traditional treatment to take into account the fact that wavepackets are not eigenstates of the Hamiltonian, as described in Sects 3.1 and 4.2 in Ref. [13]. In particular, the adiabatic transformation, of total time τ_{WP}, needs to be split into $J \sim \sqrt{\tau_{\mathrm{WP}}}$ steps and interspersed with backward time evolution to suppress the dynamical phases. This causes the adiabatic error ϵ to vanish as $J^2/\tau_{\mathrm{WP}}^2 \sim 1/\tau_{\mathrm{WP}}$ instead of as $1/\tau_{\mathrm{WP}}^2$. Our approach has the advantage that the adiabatic transformation is performed on the vacuum, rather than on the wavepackets, and there is no need to suppress the dynamical phases. To continue the discussion, we distinguish between the weak coupling regime and the strong coupling regime from now on. In both regimes we take the adiabatic paths chosen in Refs. [12,13].

A. Weak coupling

We consider scaling in the continuum limit. To determine the scaling of the time τ_{vac} required to perform the adiabatic transformation in the vacuum, we can use the analysis of adiabaticity in Sec. 4.2 in Ref. [13], taking

$J = 1$. Our setting $V = a^d \mathcal{V}$ leads to

$$\tau_{\mathrm{vac}} = \begin{cases} \tilde{O}\left(\sqrt{\dfrac{V}{\epsilon}}\right), & d = 1, 2, \\[2ex] \tilde{O}\left(\sqrt{\dfrac{V}{a^4\epsilon}}\right), & d = 3, \end{cases} \tag{69}$$

to be compared with the result obtained by Jordan, Lee, and Preskill

$$\tau_{\mathrm{WP}} = \begin{cases} \tilde{O}\left(\dfrac{V}{\epsilon}\right), & d = 1, 2, \\[2ex] \tilde{O}\left(\dfrac{V}{a^6\epsilon}\right), & d = 3. \end{cases} \tag{70}$$

We next consider the number of gates needed for the free vacuum preparation, G_{prep}, and the two kinds of adiabatic transformation, G_{WP} and G_{vac}. To this end, we take $a \sim \sqrt{\epsilon}$ and $V \sim \log_2(1/\epsilon)$, as argued in Ref. [13]. There, in Sec. 3.2, Jordan *et al.* also provide $G_{\mathrm{prep}} = \tilde{O}(1/\epsilon^{1.188d})$ and, by Eq. (68),

$$G_{\mathrm{WP}} \sim \begin{cases} \left(\dfrac{1}{\epsilon}\right)^{1.5+o(1)}, & d = 1, \\[2ex] \left(\dfrac{1}{\epsilon}\right)^{2+o(1)}, & d = 2, \\[2ex] \left(\dfrac{1}{\epsilon}\right)^{5.5+o(1)}, & d = 3. \end{cases} \tag{71}$$

Following the same reasoning, we find

$$G_{\mathrm{vac}} \sim \begin{cases} \left(\dfrac{1}{\epsilon}\right)^{1+o(1)}, & d = 1, \\[2ex] \left(\dfrac{1}{\epsilon}\right)^{1.5+o(1)}, & d = 2, \\[2ex] \left(\dfrac{1}{\epsilon}\right)^{3+o(1)}, & d = 3. \end{cases} \tag{72}$$

We see that G_{prep} dominates over G_{vac} for all the dimensions.

The advantage obtained by avoiding the adiabatic transformation on wavepackets is partially spoiled by the fact that the wavepacket creation does not succeed with a probability of 1. For simplicity, we consider two similar wavepackets, so, by Eq. (66) (replacing $\mathcal{V}$ with $\sqrt{\mathcal{V}}$ in weakly coupled ϕ^4 theory), we find that the probability

goes as

$$\rho \gtrsim \left(\frac{a^{d-1}\delta_p^d}{\sqrt{\mathcal{V}}E\bar{E}} \right)^2. \tag{73}$$

This means that we need to repeat the state preparation

$$O\left(\frac{1}{\rho}\right) = \tilde{O}\left(\frac{V}{a^{3d-2}}\right) \tag{74}$$

times to obtain the correct initial state. Notice that the LDL decomposition of the covariance matrix does not need to be repeated every time, so the total complexity of the state preparation protocol proposed here is obtained by multiplying the depth of the free vacuum preparation by $1/\rho$, which gives

$$G = \tilde{O}\left(\frac{\mathcal{V}^2}{\rho}\right) \sim \begin{cases} \left(\frac{1}{\epsilon}\right)^{1.5+o(1)}, & d=1, \\ \left(\frac{1}{\epsilon}\right)^{4+o(1)}, & d=2, \\ \left(\frac{1}{\epsilon}\right)^{6.5+o(1)}, & d=3, \end{cases} \tag{75}$$

with depth given by $\tilde{O}(\mathcal{V}^2) = \tilde{O}(1/\epsilon^d)$. The total complexity can be improved at the expense of a larger depth by use of amplitude amplification, in which case we have

$$G' = \tilde{O}\left(\frac{\mathcal{V}^2}{\sqrt{\rho}}\right) \sim \begin{cases} \left(\frac{1}{\epsilon}\right)^{1.25+o(1)}, & d=1, \\ \left(\frac{1}{\epsilon}\right)^{3+o(1)}, & d=2, \\ \left(\frac{1}{\epsilon}\right)^{4.75+o(1)}, & d=3. \end{cases} \tag{76}$$

For a direct comparison, the total complexity of the JLP algorithm is given by

$$G_{\text{JLP}} \sim \begin{cases} \left(\frac{1}{\epsilon}\right)^{1.5+o(1)}, & d=1, \\ \left(\frac{1}{\epsilon}\right)^{2.376+o(1)}, & d=2, \\ \left(\frac{1}{\epsilon}\right)^{5.5+o(1)}, & d=3. \end{cases} \tag{77}$$

B. Strong coupling

Because of the triviality issue of the ϕ^4 theory in a three-dimensional space, we can have strong coupling only for

$d=1,2$, when we approach the phase transition. For the success probability, we take

$$\rho \gtrsim \left(\frac{a^{d-1}\delta_p^d}{\mathcal{V}E\bar{E}} \right)^2. \tag{78}$$

We limit our discussion to the scaling of complexity with the coupling strength and the momenta of the incoming particle. If the phase transition occurs at the critical value λ_c, we can take $|\lambda_0 - \lambda_c|$ as a measure of the coupling strength. To estimate the scaling of the adiabatic time with this quantity, we use the results in Ref. [86], implying $\tau_{\text{vac}} \sim 1/m^3$. The temporal size T of the wavepacket ψ in Eq. (33), which determines the duration of the time evolution required to create the wavepacket in our approach, grows at most as $1/m$, by the uncertainty principle, so τ_{vac} dominates over T. Near the phase transition, the physical mass vanishes as

$$m \sim \begin{cases} \lambda_c - \lambda_0, & d=1, \\ (\lambda_c - \lambda_0)^{0.63}, & d=2, \end{cases} \tag{79}$$

which gives

$$\tau_{\text{vac}} \sim \begin{cases} \left(\frac{1}{\lambda_c - \lambda_0}\right)^3, & d=1, \\ \left(\frac{1}{\lambda_c - \lambda_0}\right)^{1.89}, & d=2. \end{cases} \tag{80}$$

Furthermore, the probability of success (78) does not depend explicitly on the mass gap. However, the volume has to be large enough to contain the wavepackets, which in turn have linear size proportional to $1/m$; hence,

$$V \sim \begin{cases} \frac{1}{\lambda_c - \lambda_0}, & d=1, \\ \left(\frac{1}{\lambda_c - \lambda_0}\right)^{1.26}, & d=2. \end{cases} \tag{81}$$

Considering the volume dependence in Eq. (68), the adiabatic transformation has a stronger scaling than the free vacuum preparation. Taking into account the success probability (78), we find that, at fixed a and incoming momenta, the total complexity scales with the coupling strength as

$$G_{\text{strong}} \sim \begin{cases} \left(\frac{1}{\lambda_c - \lambda_0}\right)^{6+o(1)}, & d=1, \\ \left(\frac{1}{(\lambda_c - \lambda_0)}\right)^{5.67+o(1)}, & d=2. \end{cases} \tag{82}$$

Using amplitude amplification, we have

$$
G'_{\text{strong}} \sim
\begin{cases}
\left(\dfrac{1}{\lambda_c - \lambda_0}\right)^{5+o(1)}, & d = 1, \\[2ex]
\left(\dfrac{1}{(\lambda_c - \lambda_0)}\right)^{4.41+o(1)}, & d = 2.
\end{cases}
\tag{83}
$$

The corresponding result found in Refs. [12,13] is

$$
G_{\text{strong,JLP}} \sim
\begin{cases}
\left(\dfrac{1}{\lambda_c - \lambda_0}\right)^{9+o(1)}, & d = 1, \\[2ex]
\left(\dfrac{1}{(\lambda_c - \lambda_0)}\right)^{6.3+o(1)}, & d = 2.
\end{cases}
\tag{84}
$$

Finally, we consider scaling with incoming momenta, at fixed coupling strength and volume. The free vacuum preparation and the adiabatic transformation in the vacuum do not depend explicitly on the incoming momenta, but the lattice spacing has to be small enough to contain momentum mode p. With $a \sim 1/p$, the free vacuum preparation has a cost proportional to p^{2d}, while the adiabatic transformation has a slower growth. The time evolution required for the wavepacket creation has a cost count of $(\mathcal{V}T)^{1+o(1)} \sim p^{d+1+o(1)}$, since T grows at most linearly with p. The success probability (78) has scaling p^{4d+2}. Putting all this together, we find the scaling

$$
G_{\text{strong}} \sim
\begin{cases}
p^{8+o(1)}, & d = 1, \\
p^{14+o(1)}, & d = 2
\end{cases}
\tag{85}
$$

or, using amplitude amplification,

$$
G'_{\text{strong}} \sim
\begin{cases}
p^{5+o(1)}, & d = 1, \\
p^{9+o(1)}, & d = 2.
\end{cases}
\tag{86}
$$

The corresponding result in Refs. [12,13] is

$$
G_{\text{strong,JLP}} \sim
\begin{cases}
p^{4+o(1)}, & d = 1, \\
p^{6+o(1)}, & d = 2.
\end{cases}
\tag{87}
$$

The scaling with the spread of the wavepackets in momentum space, δ_p, can be obtained in a similar way. In this case, we take $V \sim 1/\delta_p^d$, while we keep a fixed. The total scaling is give by

$$
G_{\text{strong}} \sim \left(\frac{1}{\delta_p}\right)^{6d+o(1)},
\tag{88}
$$

which can be improved to

$$
G'_{\text{strong}} \sim \left(\frac{1}{\delta_p}\right)^{4d+o(1)}
\tag{89}
$$

with use of amplitude amplification.

V. CONCLUSIONS

In this paper we provide a quantum algorithm to create single-particle wavepackets of a lattice quantum field theory starting from the vacuum state. The method we propose is quite general and the idea is independent of details of the model. For example, it works equally well for free and interacting theories. The key aspect of our strategy is that it is suitable for preparation of composite particles, which is an important novelty in the context of quantum simulation of relativistic scattering. To our knowledge this is the first work on state preparation of bound states for digital quantum simulation of scattering.

The work is based on the Haag-Ruelle scattering theory in the framework of axiomatic quantum field theory, which is ideal for quantum simulation as it is developed in the operator formalism. In this respect, this work also shows the potential importance that the axiomatic approach might have for quantum computation applied to quantum field theory, as both fields are suited to nonperturbative investigations from first principles. The Haag asymptotic theorem 1 provides a strong limit to obtain scattering states, rather than a weak limit as is the case in the more famous LSZ approach. This feature is what makes the Haag-Ruelle framework particularly suitable for quantum simulation, together with the fact that the convergence rate of the strong limit is very fast, as discussed after Theorem 1.

Our present result shows the potential of the Haag-Ruelle formalism in the context of quantum simulation. Here we decided to use LCU because it seems to us the easiest and most natural route, but there may be other, more efficient techniques in the context of digital quantum computation or in other contexts. Excluding the steps of vacuum preparation, and of time evolution and measurement, our algorithm requires a number of qubits that grows logarithmically with the size of the wavepacket, and a circuit depth equivalent to that of the time evolution. It succeeds with a probability that vanishes polynomially in the continuum limit for highly energetic processes and for narrow wavepackets in momentum space. The size of the mass gap is relevant only because the extension of the wavepacket in the time coordinate is inversely proportional to the mass gap.

This work decomposes the problem of state preparation for scattering into more approachable ones. On one hand, efficient techniques to prepare the vacuum state are required. On the other hand, one has to find interpolating operators with the correct properties for a given particle in a given theory, and one needs to know the size of the corresponding lower and upper mass gaps. On the first front, much work has already been done in the context of quantum computation, and we propose a way to prepare the interacting vacuum by an adiabatic transformation. We found that a scattering protocol based on creating wavepackets from the adiabatically prepared vacuum is in

some cases more efficient than the protocol proposed by Jordan *et al.* [12,13]. For the second front, standard techniques of Euclidean lattice field theory are available. As a next step, the approach of this work needs to be specialized case by case. Also, we need to investigate how gauge invariance and the presence of massless particles affect this approach.

In the last stages of the present work, we became aware of two new preprints [87,88], where similar problems are addressed with different approaches.

APPENDIX

Considering that the probability distribution determined by ψ_E in Eq. (60) is concentrated in the classically allowed region, the bound Eq. (59) seems loose, and we now explore this idea in more detail. We take a potential of the form

$$V(\phi_1,\ldots,\phi_{\mathcal{V}}) = \tilde{V}(\phi_1,\ldots,\phi_{\mathcal{V}}) + \frac{1}{a^2}\sum_{<j,j'>}\left(\phi_j - \phi_{j'}\right)^2,$$

$$\tag{A1}$$

$$\tilde{V}(\phi_1,\ldots,\phi_{\mathcal{V}}) = \sum_{j=1}^{\mathcal{V}} v(\phi_j),$$

$$\tag{A2}$$

where the summation in Eq. (A1) runs over nearest-neighbor pairs on the lattice and $v(\phi)$ is a polynomial bounded from below like $\lambda_0\phi^4 + m_0^2\phi^2$. Let cube($\phi$) denote the $\mathcal{V}$-dimensional hypercube centered at the origin and of linear size $2\phi > 0$. Let ϕ_{cl} be the smallest ϕ such that cube(ϕ_{cl}) contains the region $\tilde{V}(\phi_1,\ldots,\phi_{\mathcal{V}}) < E$ (ϕ_{cl} would be enough to describe the entire classical dynamics). Our aim here is to show that

$$\phi_{\max} = O\left(\phi_{\mathrm{cl}} + \log_2\left(\frac{\mathcal{V}}{\epsilon_{\mathrm{trunc}}}\right)\right).$$

$$\tag{A3}$$

The terms in the summation in Eq. (A1) are positive semidefinite, which implies that the classically allowed region of V is contained in the classical region of $\tilde{V}$ for all energies. Moreover, as $V \geq \tilde{V}$, the decay of the wave function outside the classical region should also be no slower for V than for $\tilde{V}$ [89]. Therefore, for our purposes, it is enough to consider $\tilde{V}$.

As $\tilde{V}$ does not contain mixing terms between different sites, we roughly approximate

$$\psi_E(\phi_1,\ldots,\phi_{\mathcal{V}}) \sim \frac{1}{\sqrt{A}}\psi_1(\phi_1)\cdots\psi_1(\phi_{\mathcal{V}}),$$

$$\tag{A4}$$

where $\psi_1(\phi_{\mathrm{cl}}) = 1$ and $\psi_1(\phi)$ rapidly decreases for $\phi > \phi_{\mathrm{cl}}$ (for a quadratic v, ψ_1 decays like a Gaussian times a polynomial). We also set

$$u(\phi) = \int_{-\phi}^{\phi} |\psi_1(\tilde{\phi})|^2 d\tilde{\phi}.$$

$$\tag{A5}$$

The normalization constant A is fixed by our requiring

$$\int_{\mathbb{R}^{\mathcal{V}}} d^{\mathcal{V}}\phi\,\frac{1}{A}|\psi_1(\phi_1)\cdots\psi_1(\phi_{\mathcal{V}})|^2 = 1,$$

$$\tag{A6}$$

which gives $A = u(+\infty)^{\mathcal{V}}$. Now we take $\phi_{\max} > \phi_{\mathrm{cl}}$, and we consider

$$\overline{\mathrm{cube}(\phi_{\max})} = \mathbb{R}^{\mathcal{V}} \setminus \mathrm{cube}(\phi_{\max}).$$

$$\tag{A7}$$

The error due to truncation $\epsilon_{\mathrm{trunc}}$ corresponds to the integral of $|\psi_E|^2$ over $\overline{\mathrm{cube}(\phi_{\max})}$. Using

$$\int_{\overline{\mathrm{cube}(\phi_{\max})}} = \int_{\mathbb{R}^{\mathcal{V}}} - \int_{\mathrm{cube}(\phi_{\max})},$$

$$\tag{A8}$$

we find

$$\begin{aligned}\epsilon_{\mathrm{trunc}} &= \int_{\overline{\mathrm{cube}(\phi_{\max})}} d^{\mathcal{V}}\phi\,\frac{1}{A}|\psi_1(\phi_1)\cdots\psi_1(\phi_{\mathcal{V}})|^2 \\ &= 1 - \left[\frac{u(\phi_{\max})}{u(+\infty)}\right]^{\mathcal{V}} \\ &= 1 - \left[1 - \frac{u(+\infty) - u(\phi_{\max})}{u(+\infty)}\right]^{\mathcal{V}}\end{aligned}$$

$$\tag{A9}$$

From the definition of an exponential,

$$e^x \approx \left(1 + \frac{x}{\mathcal{V}}\right)^{\mathcal{V}},$$

$$\tag{A10}$$

it is enough to take

$$\frac{u(+\infty) - u(\phi_{\max})}{u(+\infty)} = O\left(\frac{\epsilon_{\mathrm{trunc}}}{\mathcal{V}}\right)$$

$$\tag{A11}$$

to ensure Eq. (A9) holds. Since $\psi_1(\phi)$ vanishes exponentially or faster than $\phi \to +\infty$, so does $u(+\infty) - u(\phi_{\max})$ as $\phi_{\max} \to +\infty$, and we obtain Eq. (A3).

As a next step we would need to determine the relation between ϕ_{cl} and σ_E. While it is clear that

$$\sigma_E = O(\phi_{\mathrm{cl}} + \log_2 \mathcal{V}), \tag{A12}$$

ϕ_{cl} may be asymptotically much larger than σ_E and the form of the potential plays an important role. To see what ϕ_{cl} looks like, and to compare Eq. (A3) with Eq. (59), we focus on a more specific example—namely, the ϕ^4 theory at energy $E = O(1)$. We have

$$v(\phi) = a^d \left(\lambda_0 \phi^4 + m_0^2 \phi^2 \right). \tag{A13}$$

It can be shown that

$$\phi_{\mathrm{cl}} = \sqrt{\frac{-m_0^2 + \sqrt{4a^{-d}\lambda_0 E + \mathcal{V}m_0^4}}{2\lambda_0}}, \quad m_0^2 < 0, \tag{A14}$$

$$\phi_{\mathrm{cl}} = \sqrt{\frac{-m_0^2 + \sqrt{4a^{-d}\lambda_0 E + m_0^4}}{2\lambda_0}}, \quad m_0^2 > 0. \tag{A15}$$

In the continuum limit in the perturbative regime we have [12,13]

$$m_0^2 = \tilde{O}\left(\frac{1}{a^{d-1}}\right), \tag{A16}$$

$$\lambda_0 = \tilde{O}(1), \tag{A17}$$

$$m_0^2 < 0, \tag{A18}$$

so

$$\phi_{\mathrm{cl}} = \tilde{O}\left(\frac{\mathcal{V}^{1/4}}{a^{(d-1)/2}}\right). \tag{A19}$$

On the other hand,

$$\sigma_0 = \tilde{O}\left(\sqrt{\frac{Z}{a^{d-1}}}\right), \tag{A20}$$

and from comparison with Eq. (A19), we obtain

$$\phi_{\mathrm{cl}} = \tilde{O}\left(\frac{\mathcal{V}^{1/4}}{Z^{1/2}}\sigma_0\right). \tag{A21}$$

Provided Z is nonvanishing, we see that this result leads to a quadratic improvement in $\mathcal{V}$ with respect to the more general bound (61).

---

[1] C. W. Bauer, *et al.*, Quantum simulation for high-energy physics, PRX Quantum **4**, 027001 (2023).

[2] T. Felser, M. Trenti, L. Sestini, A. Gianelle, D. Zuliani, D. Lucchesi, and S. Montangero, Quantum-inspired machine learning on high-energy physics data, npj Quantum Inf. **7**, 111 (2021).

[3] D. Pires, Y. Omar, and J. Seixas, Adiabatic quantum algorithm for multijet clustering in high energy physics, Phys. Lett. B **843**, 138000 (2023).

[4] D. Pires, P. Bargassa, J. Seixas, and Y. Omar, A digital quantum algorithm for jet clustering in high-energy physics, ArXiv:2101.05618 (2021).

[5] D. Magano, A. Kumar, M. Kālis, A. Locāns, A. Glos, S. Pratapsi, G. Quinta, M. Dimitrijevs, A. Rivošs, P. Bargassa, J. Seixas, A. Ambainis, and Y. Omar, Quantum speedup for track reconstruction in particle accelerators, Phys. Rev. D **105**, 076012 (2022).

[6] P. Bargassa, T. Cabos, A. C. O. Choi, T. Hessel, and S. Cavinato, Quantum algorithm for the classification of supersymmetric top quark events, Phys. Rev. D **104**, 096004 (2021).

[7] A. Delgado, *et al.*, Quantum computing for data analysis in high energy physics, ArXiv:2203.08805 (2022).

[8] V. Belis, S. González-Castillo, C. Reissel, S. Vallecorsa, E. F. Combarro, G. Dissertori, and F. Reiter, Higgs analysis with quantum classifiers, EPJ Web Conf. **251**, 03070 (2021).

[9] J. Schuhmacher, L. Boggia, V. Belis, E. Puljak, M. Grossi, M. Pierini, S. Vallecorsa, F. Tacchino, P. Barkoutsos, and I. Tavernelli, Unravelling physics beyond the standard model with classical and quantum anomaly detection, Mach. Learn.: Sci. Technol. **4**, 045031 (2023).

[10] K. A. Woźniak, V. Belis, E. Puljak, P. Barkoutsos, G. Dissertori, M. Grossi, M. Pierini, F. Reiter, I. Tavernelli, and S. Vallecorsa, Quantum anomaly detection in the latent space of proton collision events at the LHC, ArXiv:2301.10780 (2023).

[11] A. Crippa, L. Funcke, T. Hartung, B. Heinemann, K. Jansen, A. Kropf, S. Kühn, F. Meloni, D. Spataro, C. Tüysüz, and Y. C. Yap, Quantum algorithms for charged particle track reconstruction in the LUXE experiment, Comput. Softw. Big Sci. **7**, 14 (2023).

[12] S. P. Jordan, K. S. M. Lee, and J. Preskill, Quantum algorithms for quantum field theories, Science **336**, 1130 (2012).

[13] S. P. Jordan, K. S. M. Lee, and J. Preskill, Quantum computation of scattering in scalar quantum field theories, Quantum Inf. Comput. **14**, 1014 (2014).

[14] S. P. Jordan, K. S. M. Lee, and J. Preskill, Quantum algorithms for fermionic quantum field theories, ArXiv:1404.7115 (2014).

[15] J. Preskill, Simulating quantum field theory with a quantum computer, ArXiv:1811.10085 (2018).

[16] G. Magnifico, M. Dalmonte, P. Facchi, S. Pascazio, F. V. Pepe, and E. Ercolessi, Real time dynamics and confinement in the $\mathbb{Z}_n$ Schwinger-Weyl lattice model for 1+1 QED, Quantum **4**, 281 (2020).

[17] A. Avkhadiev, P. E. Shanahan, and R. D. Young, Accelerating lattice quantum field theory calculations via interpolator optimization using noisy intermediate-scale quantum computing, Phys. Rev. Lett. **124**, 080501 (2020).

[18] A. Avkhadiev, P. E. Shanahan, and R. D. Young, Strategies for quantum-optimized construction of interpolating operators in classical simulations of lattice quantum field theories, Phys. Rev. D **107**, 054507 (2023).

[19] N. Klco, M. J. Savage, and J. R. Stryker, SU(2) non-Abelian gauge field theory in one dimension on digital quantum computers, Phys. Rev. D **101**, 074512 (2020).

[20] N. Mueller, A. Tarasov, and R. Venugopalan, Deeply inelastic scattering structure functions on a hybrid quantum computer, Phys. Rev. D **102**, 016007 (2020).

[21] M. Kreshchuk, W. M. Kirby, G. Goldstein, H. Beauchemin, and P. J. Love, Quantum simulation of quantum field theory in the light-front formulation, Phys. Rev. A **105**, 032418 (2022).

[22] J. F. Haase, L. Dellantonio, A. Celi, D. Paulson, A. Kan, K. Jansen, and C. A. Muschik, A resource efficient approach for quantum and classical simulations of gauge theories in particle physics, Quantum **5**, 393 (2021).

[23] M. Echevarria, I. Egusquiza, E. Rico, and G. Schnell, Quantum simulation of light-front parton correlators, Phys. Rev. D **104**, 014512 (2021).

[24] W. Qian, R. Basili, S. Pal, G. Luecke, and J. P. Vary, Solving hadron structures using the basis light-front quantization approach on quantum computers, Phys. Rev. Res. **4**, 043193 (2022).

[25] C. W. Bauer, B. Nachman, and M. Freytsis, Simulating collider physics on quantum computers using effective field theories, Phys. Rev. Lett. **127**, 212001 (2021).

[26] Y. Y. Atas, J. Zhang, R. Lewis, A. Jahanpour, J. F. Haase, and C. A. Muschik, SU(2) hadrons on a quantum computer via a variational approach, Nat. Commun. **12**, 6499 (2021).

[27] T. D. Cohen, H. Lamm, S. Lawrence, and Y. Yamauchi, Quantum algorithms for transport coefficients in gauge theories, Phys. Rev. D **104**, 094514 (2021).

[28] T. F. Stetina, A. Ciavarella, X. Li, and N. Wiebe, Simulating effective QED on quantum computers, Quantum **6**, 622 (2022).

[29] A. Kan and Y. Nam, Lattice Quantum chromodynamics and electrodynamics on a universal quantum computer, ArXiv:2107.12769 (2022).

[30] L. Funcke, T. Hartung, K. Jansen, S. Kühn, M. Schneider, P. Stornati, and X. Wang, Towards quantum simulations in particle physics and beyond on noisy intermediate-scale quantum devices, Philos. Trans. R. Soc. A **380**, 20210062 (2021).

[31] C. W. Bauer and D. M. Grabowska, Efficient representation for simulating $U(1)$ gauge theories on digital quantum computers at all values of the coupling, Phys. Rev. D **107**, L031503 (2023).

[32] A. M. Czajka, Z.-B. Kang, H. Ma, and F. Zhao, Quantum simulation of chiral phase transitions, J. High Energy Phys. **2022**, 209 (2022).

[33] D. González-Cuadra, T. V. Zache, J. Carrasco, B. Kraus, and P. Zoller, Hardware efficient quantum simulation of non-Abelian gauge theories with qudits on Rydberg platforms, Phys. Rev. Lett. **129**, 160501 (2022).

[34] Y. Y. Atas, J. F. Haase, J. Zhang, V. Wei, S. M. L. Pfaendler, R. Lewis, and C. A. Muschik, Simulating one-dimensional quantum chromodynamics on a quantum computer: Real-time evolutions of tetra- and pentaquarks, Phys. Rev. Res. **5**, 033184 (2023).

[35] R. C. Farrell, I. A. Chernyshev, S. J. M. Powell, N. A. Zemlevskiy, M. Illa, and M. J. Savage, Preparations for quantum simulations of quantum chromodynamics in $1 + 1$

dimensions. I. Axial gauge, Phys. Rev. D **107**, 054512 (2023).

[36] R. C. Farrell, I. A. Chernyshev, S. J. M. Powell, N. A. Zemlevskiy, M. Illa, and M. J. Savage, Preparations for quantum simulations of quantum chromodynamics in $1 + 1$ dimensions. II. Single-baryon β-decay in real time, Phys. Rev. D **107**, 054513 (2023).

[37] Z. Davoudi, N. Mueller, and C. Powers, Towards quantum computing phase diagrams of gauge theories with thermal pure quantum states, Phys. Rev. Lett. **131**, 081901 (2023).

[38] Z. Davoudi, N. Mueller, and C. Powers, Toward exploring phase diagrams of gauge theories on quantum computers with thermal pure quantum states, ArXiv:2212.11388 (2022).

[39] A. N. Ciavarella, S. Caspar, M. Illa, and M. J. Savage, State preparation in the Heisenberg model through adiabatic spiraling, Quantum **7**, 970 (2023).

[40] D. M. Grabowska, C. Kane, B. Nachman, and C. W. Bauer, Overcoming exponential scaling with system size in Trotter-Suzuki implementations of constrained Hamiltonians: 2+1 $U(1)$ lattice gauge theories, ArXiv:2208.03333 (2023).

[41] C. Kane, D. M. Grabowska, B. Nachman, and C. W. Bauer, Efficient quantum implementation of 2+1 $U(1)$ lattice gauge theories with Gauss law constraints, ArXiv:2211.10497 (2022).

[42] C. F. Kane, D. M. Grabowska, B. Nachman, and C. W. Bauer, Overcoming exponential volume scaling in quantum simulations of lattice gauge theories, ArXiv:2212.04619 (2022).

[43] H. Lamm, S. Lawrence, and Y. Yamauchi (NuQS), Parton physics on a quantum computer, Phys. Rev. Res. **2**, 013272 (2020).

[44] B. Nachman, D. Provasoli, W. A. de Jong, and C. W. Bauer, Quantum algorithm for high energy physics simulations, Phys. Rev. Lett. **126**, 062001 (2021).

[45] E. Gustafson, Y. Zhu, P. Dreher, N. M. Linke, and Y. Meurice, Real-time quantum calculations of phase shifts using wave packet time delays, Phys. Rev. D **104**, 054507 (2021).

[46] G. Gustafson, S. Prestel, M. Spannowsky, and S. Williams, Collider events on a quantum computer, J. High Energy Phys. **2022**, 35 (2022).

[47] A. Mariani, S. Pradhan, and E. Ercolessi, Hamiltonians and gauge-invariant Hilbert space for lattice Yang-Mills-like theories with finite gauge group, Phys. Rev. D **107**, 114513 (2023).

[48] L. Funcke, T. Hartung, K. Jansen, and S. Kühn, in *Proceedings of The 39th International Symposium on Lattice Field Theory − PoS(LATTICE2022)* (Sissa Medialab, 2023).

[49] Y. Chai, A. Crippa, K. Jansen, S. Kühn, V. R. Pascuzzi, F. Tacchino, and I. Tavernelli, Entanglement production from scattering of fermionic wave packets: A quantum computing approach, ArXiv:2312.02272 (2023).

[50] M. Rigobello, S. Notarnicola, G. Magnifico, and S. Montangero, Entanglement generation in $(1 + 1)D$ QED scattering processes, Phys. Rev. D **104**, 114501 (2021).

[51] K. Marshall, R. Pooser, G. Siopsis, and C. Weedbrook, Quantum simulation of quantum field theory using continuous variables, Phys. Rev. A **92**, 063825 (2015).

[52] F. M. Surace and A. Lerose, Scattering of mesons in quantum simulators, New J. Phys. **23**, 062001 (2021).

[53] P. I. Karpov, G. Y. Zhu, M. P. Heller, and M. Heyl, Spatiotemporal dynamics of particle collisions in quantum spin chains, Phys. Rev. Res. **4**, L032001 (2022).

[54] J. Vovrosh, R. Mukherjee, A. Bastianello, and J. Knolle, Dynamical hadron formation in long-range interacting quantum spin chains, PRX Quantum **3**, 040309 (2022).

[55] R. Belyansky, S. Whitsitt, N. Mueller, A. Fahimniya, E. R. Bennewitz, Z. Davoudi, and A. V. Gorshkov, High-energy collision of quarks and mesons in the Schwinger model: From tensor networks to circuit QED, Phys. Rev. Lett. **132**, 091903 (2024).

[56] R. A. Briceño, R. G. Edwards, M. Eaton, C. González-Arciniegas, O. Pfister, and G. Siopsis, Toward coherent quantum computation of scattering amplitudes with a measurement-based photonic quantum processor, ArXiv: 2312.12613 (2023).

[57] G. K. Brennen, P. Rohde, B. C. Sanders, and S. Singh, Multiscale quantum simulation of quantum field theory using wavelets, Phys. Rev. A **92**, 032315 (2015).

[58] M. Bagherimehrab, Y. R. Sanders, D. W. Berry, G. K. Brennen, and B. C. Sanders, Nearly optimal quantum algorithm for generating the ground state of a free quantum field theory, PRX Quantum **3**, 020364 (2022).

[59] J. Barata, N. Mueller, A. Tarasov, and R. Venugopalan, Single-particle digitization strategy for quantum computation of a ϕ^4 scalar field theory, Phys. Rev. A **103**, 042410 (2021).

[60] A. Duncan, *The Conceptual Framework of Quantum Field Theory* (Oxford University Press, Oxford, United Kingdom, 2012).

[61] N. Klco and M. J. Savage, Systematically localizable operators for quantum simulations of quantum field theories, Phys. Rev. A **102**, 012619 (2020).

[62] A. C. Y. Li, A. Macridin, S. Mrenna, and P. Spentzouris, Simulating scalar field theories on quantum computers with limited resources, Phys. Rev. A **107**, 032603 (2023).

[63] D. Paulson, L. Dellantonio, J. F. Haase, A. Celi, A. Kan, A. Jena, C. Kokail, R. van Bijnen, K. Jansen, P. Zoller, and C. A. Muschik, Simulating 2D effects in lattice gauge theories on a quantum computer, PRX Quantum **2**, 030334 (2021).

[64] A. N. Ciavarella and I. A. Chernyshev, Preparation of the $SU(3)$ lattice Yang-Mills vacuum with variational quantum methods, Phys. Rev. D **105**, 074504 (2022).

[65] R. C. Farrell, M. Illa, A. N. Ciavarella, and M. J. Savage, Scalable circuits for preparing ground states on digital quantum computers: The Schwinger model vacuum on 100 qubits, ArXiv:2308.04481 (2023).

[66] T. D. Cohen and H. Oh, Efficient vacuum state preparation for quantum simulation of strongly interacting local quantum field theories, Phys. Rev. A **109**, L020402 (2024).

[67] T. Li, W. K. Lai, E. Wang, and H. Xing, Scattering amplitude from quantum computing with reduction formula, Phys. Rev. D **109**, 036025 (2024).

[68] J. Glimm and A. Jaffe, A $\lambda\phi^4$ quantum field theory without cutoffs. I, Phys. Rev. **176**, 1945 (1968).

[69] J. Glimm and A. Jaffe, The $\lambda(\varphi^4)_2$ quantum field theory without cutoffs: II. The field operators and the approximate vacuum, Ann. Math. **91**, 362 (1970).

[70] J. Glimm and A. Jaffe, The $\lambda(\varphi^4)_2$ quantum field theory without cutoffs: III. The physical vacuum, Acta Math. **125**, 203 (1970).

[71] J. Glimm and A. Jaffe, The $\lambda\varphi_2^4$ quantum field theory without cutoffs. IV. Perturbations of the Hamiltonian, J. Math. Phys. **13**, 1568 (2003).

[72] J. Glimm and A. Jaffe, Positivity of the φ_3^4 Hamiltonian, Fortschr. Phys. **21**, 327 (1973).

[73] J. Glimm, A. Jaffe, and T. Spencer, The Wightman axioms and particle structure in the $P(\varphi)_2$ quantum field model, Ann. Math. **100**, 585 (1974).

[74] J. D. Dimock and J.-P. Eckmann, On the bound state in weakly coupled $\lambda(\varphi^6 - \varphi^4)_2$, Commun. Math. Phys. **51**, 41 (1976).

[75] T. Spencer and F. Zirilli, Scattering states and bound states in $\lambda P(\phi)_2$, Commun. Math. Phys. **49**, 1 (1976).

[76] J. D. Dimock and J.-P. Eckmann, Spectral properties and bound-state scattering for weakly coupled $\lambda P(\phi)_2$ models, Ann. Phys. (N. Y.) **103**, 289 (1977).

[77] S. Bachmann, W. Dybalski, and P. Naaijkens, Lieb–Robinson bounds, Arveson spectrum and Haag–Ruelle scattering theory for gapped quantum spin systems, Ann. Henri Poincaré **17**, 1737 (2016).

[78] J. C. A. Barata and K. Fredenhagen, Particle scattering in Euclidean lattice field theories, Commun. Math. Phys. **138**, 507 (1991).

[79] N. Klco and M. J. Savage, Digitization of scalar fields for quantum computing, Phys. Rev. A **99**, 052335 (2019).

[80] A. M. Childs, R. Kothari, and R. D. Somma, Quantum algorithm for systems of linear equations with exponentially improved dependence on precision, SIAM J. Comput. **46**, 1920 (2017).

[81] G. Brassard, P. Høyer, M. Mosca, and A. Tapp, in *Quantum Computation and Information (Washington, DC, 2000)*, Contemporary Mathematics, Vol. 305 (American Mathematical Society, Providence, RI, 2002), p. 53.

[82] A. M. Childs, Y. Su, M. C. Tran, N. Wiebe, and S. Zhu, Theory of Trotter error with commutator scaling, Phys. Rev. X **11**, 011020 (2021).

[83] E. Manousakis, *Practical Quantum Mechanics: Modern Tools and Applications* (Oxford University Press, Oxford, United Kingdom, 2015).

[84] A. Kitaev and W. A. Webb, Wavefunction preparation and resampling using a quantum computer, ArXiv:0801.0342 (2009).

[85] C. W. Bauer, P. Deliyannis, M. Freytsis, and B. Nachman, Practical considerations for the preparation of multivariate Gaussian states on quantum computers, ArXiv:2109.10918 (2021).

[86] S. Jansen, M.-B. Ruskai, and R. Seiler, Bounds for the adiabatic approximation with applications to quantum computation, J. Math. Phys. **48**, 102111 (2007).

[87] M. Kreshchuk, J. P. Vary, and P. J. Love, Simulating scattering of composite particles, ArXiv:2310.13742 (2023).

[88] R. C. Farrell, M. Illa, A. N. Ciavarella, and M. J. Savage, Quantum simulations of hadron dynamics in the Schwinger model using 112 qubits, ArXiv:2401.08044 (2024).

[89] J. L. Gervais and B. Sakita, WKB wave function for systems with many degrees of freedom: A unified view of solitons and pseudoparticles, Phys. Rev. D **16**, 3507 (1977).